Meteorol. Zeitschrift, N.F. 7, 181–187 (August 1998)

How the sky gets covered with condensation trails

KLAUS GIERENS, Oberpfaffenhofen

Summary. Simple numerical principle studies are presented that investigate the growth of a contrail sheet under the influence of wind shear, cross-wind, and air traffic density. It is assumed that ambient conditions allow contrails to persist for a couple of hours without sedimentation. Three growth regimes of a contrail sheet are found: an initial regime of diffusional growth, a second regime of shear-driven growth, and a mature stage without further growth which is reached either by approaching overcast conditions or earlier with fractional coverage far from overcast sky, when the contrails are driven away from the considered region by a strong cross-wind or when they get sub-visible because of too little humdity available in the environment.

Die Bedeckung des Himmels mit Kondensstreifen

Zusammenfassung. Es werden einfache numerische Prinzipstudien vorgestellt, mit denen die allmähliche Bedeckung des Himmels mit Kondensstreifen unter dem Einfluß von Windscherung, Querwind und Verkehrsdichte untersucht wird. Es wird vorausgesetzt, daß die Umgebungsbedingungen die mehrstündige Persistenz der Kondensstreifen erlauben, ohne daß es zur Sedimentation kommt. Es sind drei Phasen zu unterscheiden: zuerst steigt die Bedeckung durch die Ausbreitung einzelner Kondensstreifen durch Diffusion an, danach übernimmt die Windscherung die dominierende Rolle. Schließlich wird ein Reifestadium erreicht, in dem der Bedeckungsgrad nicht weiter ansteigt. Dieses Stadium wird entweder bei vollständiger Bedeckung erreicht oder schon früher, wenn entweder ein kräftiger Querwind die Kondensstreifen aus dem betrachteten Gebiet heraustreibt, oder diese wegen zu geringen Feuchteangebots der Umgebungsluft immer optisch dünner und schließlich unsichtbar werden.

1. Introduction

The impact of aviation emissions upon the atmosphere is considered at present a very important issue that receives attention by scientists, aircraft manufacturers, airlines, and policy makers. Currently, the IPCC (International Panel on Climate Change) is writing a special report on the aviation impact on climate. The state of knowledge has been reviewed recently by BRASSEUR et al. (1998).

Condensation trails (contrails) are the most obvious effect of cruising air traffic in the atmosphere. Like natural clouds, they modify the radiation budget of the Earth-atmosphere system. In view of the large present-day and predicted future growth rates of air traffic, the question arises whether the enhancement of high cloudiness by contrails may have a climatological impact. The potential of a significant climate change due to contrails has been demonstrated by PONATER et al. (1996) who used a general circulation model in which they introduced additional high cloudiness due to contrails.

The thermodynamic theory of contrail formation has been reviewed recently by SCHUMANN (1996): According to the theory of SCHMIDT (1941) and APPLEMAN (1953) contrails are formed when water saturation is reached in the exhaust plume during the mixing of the hot and humid exhaust air with the cold ambient air. If this occurs, the vapour condenses first into liquid droplets and may later freeze. If the ambient air is supersaturated with respect to ice the new contrail can persist for a long time. A recent flight experiment during the SUCCESS campaign (MINNIS et al. 1998) has demonstrated that a persistent contrail can last for hours. During its lifetime a contrail grows by diffusion and wind shear. After a while it does no longer give the impression of a line cloud, rather it has spread out so much that it is difficult do distinguish it from natural cirrus (SCHUMANN and WENDLING 1990). In particular in the case of contrail sheets, which is a field of many contrails that spread out and interlace until they eventually form an apparent sheet cloud (e.g. KUHN 1970), the distinction between contrails and natural cirrus becomes extremely difficult, if not impossible at all. How rapid a contrail sheet evolves depends on the air traffic density and on the spreading rate of a single contrail.

For an assessment of the potential of contrails to change the climate (globally and regionally) it is an essential prerequisite to determine the status quo, i.e. to set up a present-day contrail climatology. Regional contrail climatologies have been obtained for Europe by evaluation of satellite pictures, both interactively (e.g. BAKAN et al. 1994) and automatically (MANNSTEIN 1996, MANNSTEIN et al. 1997). Contrail climatologies for the USA have been obtained by direct observations from US Air Force crews (PETERS 1993) and by ground-based observations (MINNIS et al. 1997). A global contrail climatology is set up currently by SAUSEN et al. (1998) who evaluate a global air traffic inventory (SCHMITT and BRUNNER 1997) together with meteorological data from the ECMWF re-analysis project (GIBSON et al. 1997). Such a work is subject to the problem

0941-2948/98/0007-0181 $ 03.15

that the contrail coverage over a region is not necessarily proportional to the air traffic density. Saturation effects due to the evolution of contrail sheets (contrail overlapping and approach of overcast sky) are the origin of the non-linearity.

The aim of the present study is the investigation of the development of contrail sheets and the mentioned saturation effects under the influence of several factors, viz. wind shear, cross-wind, contrail lifetime, and traffic density. To this end, simple numerical simulations have been performed that demonstrate how the sky — e.g. in the region of a flight corridor — gets covered with contrails. It is not the aim of the present paper to show detailed numerical simulations of the evolution of single contrails, including their microphysical properties. Such a study (which serves other purposes) has been published elsewhere (GIERENS 1996). In the following Section 2 I describe the method, then I present some results of principle studies in Section 3, the result of a more realistic case follows in Section 4, and finally, conclusions are drawn in Section 5.

2. Method

The method used here is similar to the method of SCHUMANN and KONOPKA (1994) who investigated how NO_x is distributed throughout an air corridor in a period of a few days.

Consider a control plane (Fig. 1) of width W (1000 km for the North-Atlantic flight corridor, 100 km for a regional air route) and height H (typically 4 km, covering the altitude range of cruise levels, i.e. 8–12 km). The control area is placed perpendicular to the considered air route. Aircraft cross the control area plus two stripes at the lateral borders (for allowance of drift in and out) at uniformly distributed random positions (this might be an idealization), whereas the arrival times are simulated according to a Poisson process (see, e.g., GOODMAN 1988). The Poisson process is a random process where the number of events that occur during a certain period Δt is randomly distributed according to a Poisson law with mean $\lambda \cdot \Delta t$. The rate λ of the Poisson process is a measure of traffic intensity, i.e. number of aircraft arriving in a certain time interval. In reality, λ is a function of time (non-homogeneous Poisson process), since the traffic intensity has a diurnal variation. Such a situation will be considered in Section 4. However, for the following principle studies, a homogeneous Poisson process with constant rate will be assumed, i.e. a non-varying traffic intensity. Some typical realizations of a homogeneous Poisson process are depicted in Fig. 2.

Microphysical phenomena like contrail formation, ice production, and sedimentation, are not considered in the present study. Instead, it is simply assumed that ambient conditions allow contrails to persist for a couple of hours without developing precipitation. The ambient relative humidity is assumed to control the lifetime of the contrails. According to the concept of BOIN and LEVKOV (1994) the lifetime of a contrail ceases when its transmissivity for visible light exceeds 99.5 %. BOIN and LEVKOV showed that

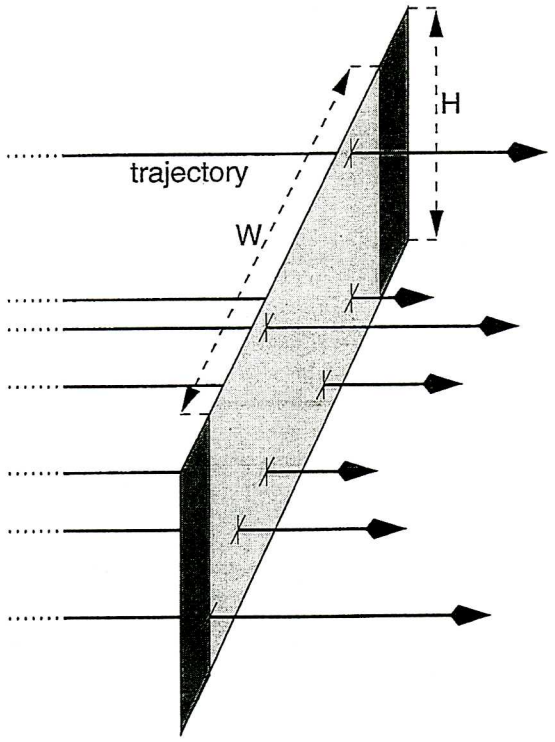

Fig. 1. A perspective view onto the control plane (light grey) used in the model, together with two side stripes (dark grey) and some sample aircraft trajectories. Note the different scales used for the vertical and horizontal dimensions: typically, W = 1000 km, whereas H = 4 km.

Abb. 1. Perspektivische Ansicht der Kontrollfläche (hellgrau) zusammen mit ihren beiden Seitenstreifen (dunkelgrau) und einigen beispielhaften Flugzeugtrajektorien. Die horizontalen und vertikalen Skalen sind verschieden: typische Werte sind W = 1000 km und H = 4 km.

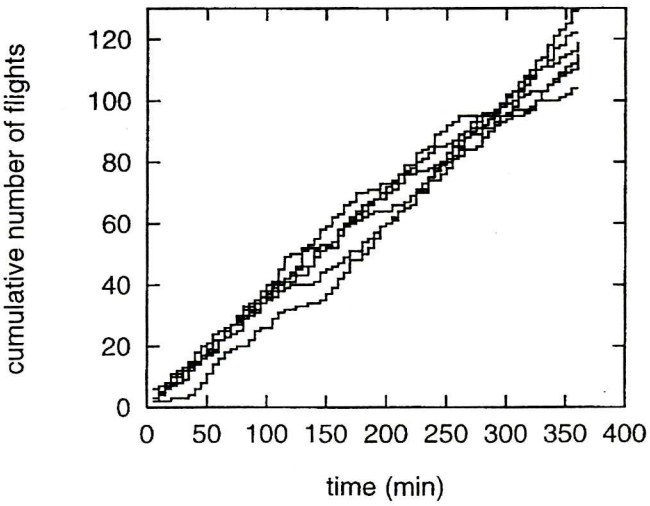

Fig. 2. Some realizations of a homogeneous Poisson process with rate $\lambda = 1/3\ \text{min}^{-1}$, i.e. on average there arrives one aircraft at the control area every three minutes.

Abb. 2. Einige Realisierungen eines Poissonprozesses mit der Rate $\lambda = 1/3\ \text{min}^{-1}$, d.h. im Mittel tritt ein Flugzeug pro 3 Minuten durch die Kontrollfläche.

the lifetime of a contrail increases exponentially with increasing ambient humidity. In their model a lifetime of 6 hours is reached at a relative humidity of 124 % with respect to ice.

The spreading of a contrail is assumed to follow the rules for a Gaussian plume (KONOPKA 1995):

$$\sigma_h^2 = 2/3 s^2 D_v t^3 + (2sD_s + s^2\sigma_{v,0}^2)t^2 + 2(s\sigma_{s,0}^2 + D_h)t + \sigma_{h,0}^2, \quad (1)$$

where the horizontal, vertical, and slanted diffusivities are: $D_h = 15\ m^2s^{-1}$, $D_v = 0.15\ m^2s^{-1}$, and $D_s = 0.4(D_hD_v)^{1/2}$. s is wind shear, and σ_h is the time-dependent horizontal standard deviation of the Gaussian plume which is identified with the lateral contrail half width (SCHUMANN et al. 1995). Initial contrail dimensions are chosen following SCHUMANN and KONOPKA (1994): $\sigma_{h,0} = 100$ m, $\sigma_{v,0} = 70$ m, and $\sigma_{s,0} = 0$. Due to cross-wind and wind shear, contrails are allowed to drift into and out from the control volume. The drift velocity is given by

$$v(z) = v(z_0) + s(z-z_0), \quad (2)$$

where $v(z_0) =: v_0$ is the cross-wind at a reference altitude z_0 (here the half height of the control volume).

The simulations begin with a clear sky and follow the evolution of the fractional contrail coverage for 6 hours. If not specified otherwise, the contrail lifetime is assumed to exceed 6 hours. The fractional contrail coverage, b, is computed by dividing the sum of the widths of the individual contrails, corrected for overlapping (i.e. overlapping pieces are counted only once), through the widht, W, of the control area. Contrails extending outside of the control area, or contrails that reach into it from the side-stripes, are counted as far they are within the borders of the control plane.

3. Principle studies

The effect of wind shear on the growth of the fractional contrail coverage is shown in Fig. 3. Simulations have been performed with wind shear between 0 and 0.02 s^{-1} ($s = 0.003\ s^{-1}$ is a typical value for the upper troposphere). For all simulations, a total of 122 aircraft have passed the control area in the considered 6 h period (which corresponds roughly to the actual situation in the North-Atlantic flight corridor), the rate of the Poisson process was $\lambda = 1/3\ min^{-1}$, the domain width was W = 1000 km, the mean cross-wind was $v_0 = 0$. As expected, the contrail coverage b grows as the air traffic is going on. Even without wind shear, b increases with time, though weakly (exclusively by horizontal diffusion of individual contrails). From Eq. (1) it is clear that the spreading of individual contrails is much more rapid with wind shear than without. This is reflected in the more rapid growth of the contrail coverage b. Generally, three periods can be distinguished. In an initial period (about 1 h) the increase of b(t) is dominated by horizontal diffusion (the term linear in t in Eq. (1)). Thereafter, the wind shear becomes important and leads to an enhanced increase rate

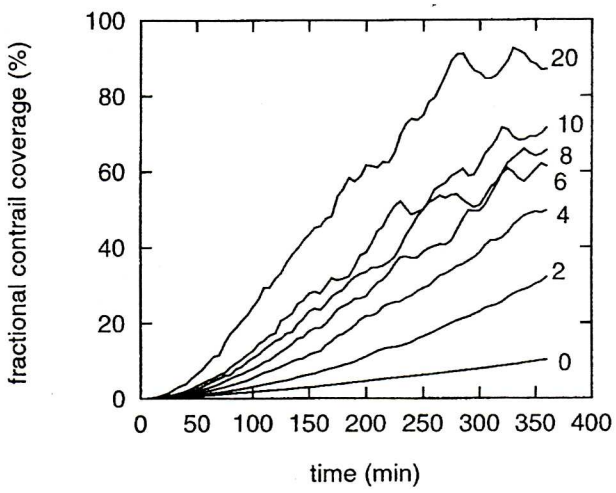

Fig. 3. Fractional coverage due to contrails vs. time in an air corridor of 1000 km width and with an arrival rate of $\lambda = 1/3\ min^{-1}$. The curve-parameter is wind shear s in units of (m/s)/km. The mean cross-wind was zero in these simulations.

Abb. 3. Bedeckungsgrad durch Kondensstreifen als Funktion der Zeit in einem 1000 km breiten Luftkorridor und mit einer Ankunftsrate von $\lambda = 1/3\ min^{-1}$. Der Kurvenparameter ist die Windscherung in Einheiten von (m/s)/km. Der mittlere Querwind ist hier 0 m/s.

of b(t). b(t) grows approximately linearly with time during this period. Finally, the sky might get overcast with contrails, which stops further growth of b. For the largest considered wind shear, this situation is reached after 5 h, and thereafter the cloudiness merely fluctuates randomly around a value of $b \approx 90$ %. Such fluctuations are common to the cases with larger wind shear ($s \gtrsim 0.006\ s^{-1}$), with wiggling increasing with wind shear. These wiggles are caused by contrails, that drift out and into the control area: If a conrail drifts out, the cloudiness in the control area is reduced, which leads to a non-monotonic increase of b(t). Saturation effects in the sense of approaching overcast conditions are not evident during the 6 h simulation period in the cases with $s \leq 0.01\ s^{-1}$. However, another kind of saturation is always present: this is saturation in the sense of overlapping of individual contrails (which might be conceived a locally overcast condition). If b is considered a function of s, then this function has a form like $b(s) \approx b(0) + [1-b(0)]\,(1-e^{-\alpha s})$, with a time-dependent parameter α. The term $1-e^{-\alpha s}$ indicates saturation.

A strong cross-wind blowing through an air route can inhibit a substantial contrail cloudiness, even when the wind shear is large and the traffic density is high. This is shown in Fig. 4, where a set of 4 simulations is used to demonstrate the influence of the cross-wind. All simulations are run with $\lambda = 1/3\ min^{-1}$ and W = 1000 km. Two different wind shears ($s = 0.002$ and $0.005\ s^{-1}$) have been used. The curves show the difference between cases without cross-wind and with a strong cross-wind of speed $v_0 = 50\ m\ s^{-1}$. It can be seen that the cross-wind inhibits the fractional contrail coverage to grow beyond a certain amount, that depends on the wind shear. The time when b ceases to grow is reached earlier in

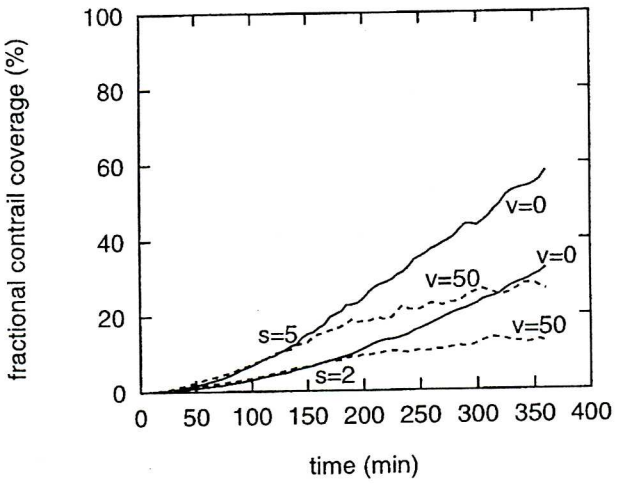

Fig. 4. Temporal evolution of contrail cloudiness in situations with strong cross-wind of v_0 = 50 ms^{-1} (dotted) or without cross-wind (solid). Wind shear s in (m/s)/km is indicated.

Abb. 4. Zeitliche Entwicklung der Bedeckung durch Kondensstreifen in Situationen mit einem kräftigen Querwind von v_0 = 50 ms^{-1} (punktiert) und ohne Querwind (durchgezogen). Die Windscherung s in (m/s)/km ist angegeben.

the case with higher wind shear (after about 2 h) as compared with the low wind shear case (after about 3 h). The maximum cross-wind speed in the control area increases with wind shear. In spite of this, the value of b that is eventually obtained is larger in the case with higher wind shear. This result is not trivial. The strong cross-wind stops the shear driven growth of the contrail sheet by establishing an equilibrium between the formation of new contrails by newly arriving aircraft and the removal of contrails when they drift out of the control area.

As noted above, a contrail's lifetime may be considered terminated when the contrail becomes transparent for visible light. Such sub-visible contrails do not contribute to fractional cloudiness as judged from a human observer. Since contrail lifetime is a steep function of ambient relative humidity (BOIN and LEVKOV 1994), it is evident that the ambient humidity has a strong influence on the temporal evolution of the fractional contrail cloudiness. In order to investigate this influence, cases have been simulated with λ = 1/3 min^{-1}, W = 1000 km, s = 0.005 s^{-1}, and a set of lifetimes T of 1, 3, and 6 h, which corresponds to relative humidities with respect to ice of 112, 119, and 124 %, respectively, according to the formula given by BOIN and LEVKOV. The result of this investigation is simple (not shown): Trivially, for simulation times t < T there is no effect of the contrail lifetime. After t = T the oldest contrails vanish with the same rate as new ones are formed (at least as long the traffic intensity is constant). Thus, for t > T the contrail coverage stays nearly constant at the value that was reached at t = T. Since the vanishing contrails are broader than the new ones, the contrail coverage actually is decreasing slightly after t = T until finally an equilibrium between contrail formation, spreading, and termination is reached.

Of course, contrail cloudiness depends on the actual traffic density and on the traffic density of the past few hours (depending on contrail lifetime) — a memory effect caused by the persistence of contrails. The notion "traffic density" has a spatial and a temporal component. The spatial component may be identified in the present context with the corridor width, W, while the temporal component is the traffic intensity, expressed via the aircraft arrival rate λ. It should be noted that the arrival rate (min^{-1}) refers to the control area, not to a unit area or length. Thus, it might be expected that the only parameter that characterizes "traffic density" is the ratio λ/W. Indeed, this expectation is confirmed by the simulations presented in Fig. 5. Two pairs of simulations with wind shears of 0.002 and 0.005 s^{-1} have been performed; in each pair the traffic density was λ/W = (1/3)/1000 and (2/3)/2000 min^{-1}/km, i.e. both corridor width and traffic intensity have been doubled simultaneously. In both pairs of simulations the temporal evolution of the contrail coverage was almost identical for both values of traffic density. The slight differences visible on Fig. 5 merely result from the different (random) Poisson processes used in the simulations.

Since traffic density can be described by λ/W, it is not necessary to consider both the influence of traffic intensity λ and corridor width W on the formation of a contrail sheet.

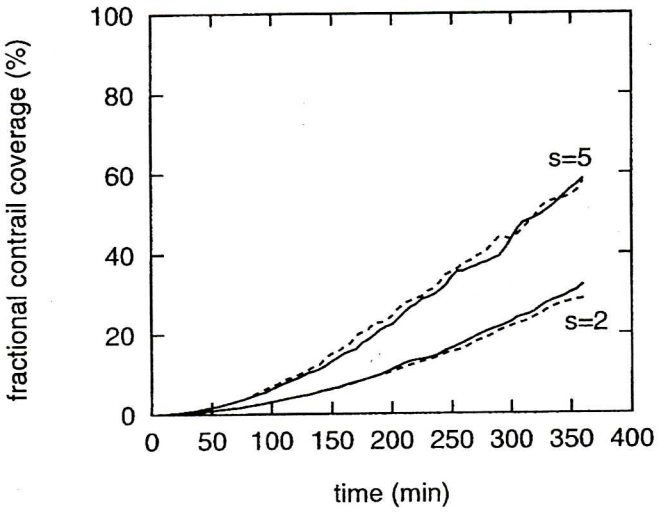

Fig. 5. Temporal evolution of contrail cloudiness in flight corridors of 1000 and 2000 km width, and with traffic intensity of 1/3 and 2/3 min^{-1}. Solid lines: λ/W = (1/3)/1000 min^{-1}/km, dotted lines: λ/W = (2/3)/2000 min^{-1}/km. If corridor width and traffic intensity are both multiplied with the same factor, the resulting b(t) curves are almost identical. Differences are merely due to the different Poisson process. Wind shear s in (m/s)/km is indicated.

Abb. 5. Zeitliche Entwicklung der Bedeckung durch Kondensstreifen in Flugkorridoren von 1000 und 2000 km Breite und mit Verkehrsintensitäten von 1/3 und 2/3 min^{-1}. Durchgezogene Linien: λ/W = (1/3)/1000 min^{-1}/km, gepunktete Linien: λ/W = (2/3)/2000 min^{-1}/km. Wenn Korridorbreite und Verkehrsintensität mit dem gleichen Faktor multipliziert werden, zeigt b(t) im wesentlichen den gleichen Verlauf. Unterschiede sind auf die verschiedenen Poissonprozesse zurückzuführen. Die Windscherung s in (m/s)/km ist angegeben.

It suffices to consider different corridor widths, and the growing contrail coverage in these corridors. A single air route may have a width of the order 100 km, while the North-Atlantic flight corridor has a width of more than 2000 km. Of course, subject to the same traffic intensity, a single air route is much earlier overcast with a contrail sheet than the North-Atlantic flight corridor. This is shown in Fig. 6a (wind shear 0.002 s^{-1}) and 6b ($s = 0.005\ s^{-1}$). In both cases no cross-wind and $\lambda = 1/3\ min^{-1}$ was assumed. In the higher wind shear case the 100 km wide air route is overcast 4 h after start of the traffic, in the case with lower wind shear overcast conditions are reached one hour later. For the wider air corridors considered in the simulations, this kind of saturation is still far away after 6 h of traffic. However, the other kind of saturation mentioned above, i.e. the growing degree of overlapping of contrails, is perceivable in the Figures: At a given time the fractional contrail coverage is a non-linear function of traffic density (i.e. of the inverse of corridor width, since λ was constant). If we write "δ" for λ/W, then a functional relation of the form $b(\delta) \approx 1-e^{-\beta\delta}$ with a time-dependent parameter β can be used to approach the fractional contrail coverage as a function of traffic density δ. Again, the functional form indicates saturation.

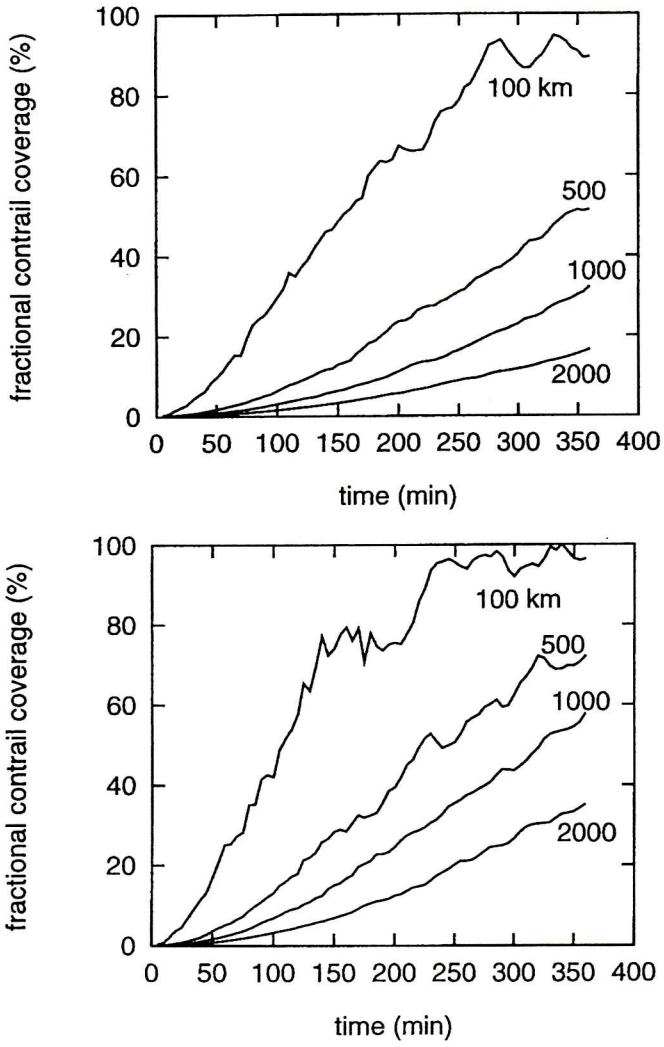

Fig. 6a. Fractional contrail cloudiness vs. time for air routes and flight corridors of different width as indicated, but with equal traffic intensity ($\lambda = 1/3\ min^{-1}$). Wind shear is 2 (m/s)/km.

Abb. 6a. Zeitliche Entwicklung der Bedeckung durch Kondensstreifen für Luftstraßen und Flugkorridore mit den angegebenen Breiten, aber mit gleicher Verkehrsintensität ($\lambda = 1/3\ min^{-1}$). Die Windscherung beträgt 2 (m/s)/km.

Fig. 6b. As Fig. 6a, but with wind shear of 5 (m/s)/km.

Abb. 6b. Wie Abb. 6a, aber mit einer Windscherung von 5 (m/s)/km.

4. A case with time-dependent traffic intensity

We consider again a 1000 km wide control area crossing the North-Atlantic flight corridor, but now we assume a time-dependent traffic intensity, i.e. $\lambda = \lambda(t)$ (this constitutes a non-homogeneous Poisson process, cf. GOODMAN 1988). $\lambda(t)$ is chosen in such away that the actual air traffic of 15 June 1989 is modelled (see Fig. 2 of SCHUMANN and KONOPKA 1994). Flight positions are still chosen randomly, as before. Although in reality flights take place on a discrete set of flight levels, the random choice of vertical flight positions does not effect the results presented in this study (since the information on the flight altitude is not used in the evaluation of b). The random choice of horizontal positions, on the other hand, could lead to a higher contrail coverage than in reality, since then contrail overlapping is smaller than with flights taking place on a few air routes inside the corridor, each only about 100 km wide. We consider cases with a wind shear of 0.005 s^{-1}, cross-winds of 0 and 50 ms^{-1}, and contrail lifetimes of 6 and 12 h. The simulations are run for 24 h, and a total of 286 aircraft pass the control area during the first 18 h of this period.

The results are shown in Fig. 7a (for $v_0 = 0\ ms^{-1}$) and 7b (for $v_0 = 50\ ms^{-1}$). During the first two hours the air traffic is very sparse ($\lambda = 0.035\ min^{-1}$). Accordingly, the contrail coverage is nearly zero. Then, the traffic intensity increases considerably and stays on large values for the next 5 h, with a maximum arrival rate of $\lambda_{max} = 0.49\ min^{-1}$. During this 5 h period we can recognize the two phases of growth of the contrail sheet: first the diffusional growth regime for about 1 h and thereafter the shear dominated growth with approximately linear (with time) growth of b(t) (cf. Section 3).

It is interesting to note that in the case without cross-wind and with 12 h lifetime the growth of b(t) does neither stop nor proceed at a significantly lower rate after 7 h of simulation, although then the traffic intensity is reduced to a low value of $\lambda = 0.07\ min^{-1}$. This is a consequence of the memory effect already mentioned: The contrails persist and grow further even hours after their producing aircraft has gone. Similarly the contrail sheet can persist and expand hours after the last producing aircaft has left the flight corridor. During the second phase of intense traffic the contrail coverage grows on and eventually reaches overcast conditions after 15 h (for $s = 0.005\ s^{-1}$). The transient decrease of b(t) between 17 and 19 h is a result of the

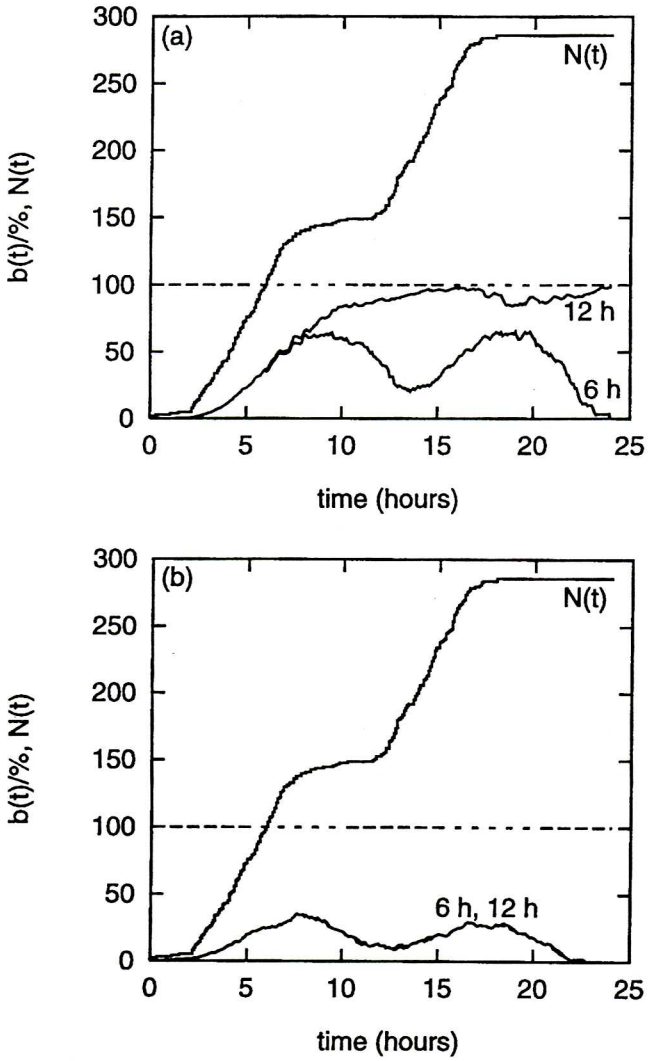

Fig. 7a. Fractional contrail coverage, b, vs. time, and accumulated number of aircraft arrived, N, vs. time in a simulation with time-varying traffic intensity. Two simulations have been performed with contrail lifetimes of 6 h (lower curve) and 12 h (upper curve). The simulations were performed without cross-wind. The wind shear was 5 (m/s)/km. The corridor width was W = 1000 km.

Abb. 7a. Zeitliche Entwicklung der Bedeckung durch Kondensstreifen, b, und aufsummierte Anzahl von Durchflügen, N, in einer Situation mit zeitlich veränderlicher Verkehrsintensität. Es wurden zwei Simulationen durchgeführt, wobei für die Lebensdauer der Kondensstreifen 6 (untere Kurve) und 12 Std. (obere Kurve) angenommen wurden. Diese Simulationen wurden ohne Querwind durchgeführt. Die Windscherung betrug 5 (m/s)/km. Der Luftkorridor war 1000 km breit.

Fig. 7b. As Fig. 7a, but with cross-wind of 50 ms^{-1}. Please note, that the two curves for contrail lifetimes of 6 and 12 hours are almost congruent.

Abb. 7b. Wie Abb. 7a, aber mit einem Querwind von 50 ms^{-1}. Man beachte, daß die beiden Kurven für die Lebensdauer von 6 und 12 Stunden nahezu kongruent sind.

assumed finite contrail lifetime of 12 h, because there is no such decrease in the contrail coverage when an infinite contrail lifetime is assumed (not shown).

In the case with shorter lifetime of 6 h (again without cross-wind) and also in the cases with strong cross-wind, a memory effect does not become operative. Instead the contrail coverage follows the traffic intensity with a certain time lag of 2 to 3 h. As a function of time, b(t) displays two maxima that correspond to the two traffic intensity maxima. The coverage maxima are reached when the traffic intensity is already back at its minimum. It is interesting to note that in the cases with strong cross-wind the resulting contrail coverages b(t) are nearly equal for both lifetime assumptions of 6 and 12 h. Both curves are congruent within the resolution of Fig. 7b. A plausible reason for this finding can be obtained by a comparison of the relevant time scales: A cross-wind time scale is given by the ratio W/v_0, which is the time needed to cross the corridor width W with a speed v_0. In the present case this time is 5.5 h which is shorter than the shortest contrail lifetime considered. Thus, in the considered cases, the contrails begin to drift away from the corridor before they become sub-visible.

5. Conclusions

Simple numerical principle studies have been performed in order to simulate the formation of contrail sheets over air routes and international flight corridors. It has been assumed that the atmosphere is moist enough to allow contrails to persist without formation of precipitation for a couple of hours. How a contrail sheet develops depends on wind shear, cross-wind, contrail lifetime, and traffic density (i.e. the ratio of traffic intensity and corridor width). Three regimes of growth of the contrail sheet can be distinguished:

1) A diffusional growth regime, during which the first relatively young contrails grow by horizontal diffusion (characterized by the turbulent horizontal diffusivity D_h, which is typically of the order 15 m^2s^{-1}). The diffusional growth regime lasts typically 1 h.

2) A shear-driven growth regime, during which the fractional contrail coverage grows approximately linearly with time. The growth rate depends on wind shear and traffic density in a non-linear way, which accounts for the second saturation effect, viz. the one caused by the overlapping of contrails.

3) The shear driven growth regime is stopped either by approaching the first kind of saturation, i.e. overcast conditions, or by a strong cross-wind or when contrails begin to become sub-visible (insufficient moisture in ambient air) far before overcast conditions are reached. In the latter cases an equilibrium is established between formation of new contrails and contrail disappearance when they either drift out of the control area or become sub-visible. It depends on the relevant time scales (lifetime vs. cross-wind time scale), which process becomes effective in stopping the growth of the contrail sheet.

The consideration of a time-varying traffic intensity does not yield results that would change any of the findings obtained from the principle studies. Instead, it provided a nice instance of the memory effect due to contrail persist-

ence when the contrail lifetime was sufficiently long: Even after a considerable reduction of traffic intensity the contrail sheet grew on with apparently the same rate as before, when there was no cross-wind.

Currently, an investigation of persistent contrail cloudiness due to present-day air traffic and climate is performed (SAUSEN et al. 1998). In such a study it is necessary to multiply a theoretical maximum fractional contrail coverage (independent of actual traffic) with a measure of traffic density (e.g. fuel consumed at a given location during a certain period). The present study indicates that it is a good choice to assume a linear weighting (i.e. contrail coverage proportional to number of aircraft), since saturation due to overcast situations (which would substantiate choice of, e.g., logarithmic weighting) are only reached in extreme situations (very high traffic density, very high wind shear).

Acknowledgment

I thank U. SCHUMANN and R. SAUSEN for critically reading the manuscript. The work has been funded by the Commission of the European Union via the project AEROCONTRAIL (contract nr. ENV4-CT95-0157).

References

Appleman, H., 1953: The formation of exhaust condensation trails by jet aircraft. — Bull. Amer. Meteor. Soc. **34**, 14–20.

Bakan, S., M. Betancor, V. Gayler, H. Graßl, 1994: Contrail frequency over Europe from NOAA-satellite images. — Ann. Geophysicae **12**, 962–968.

Boin, M., L. Levkov, 1994: Numerical simulation of the lifetime of contrails. — In: Schumann, U., D. Wurzel (Eds.): Impact of Emissions from Aricraft and Spacecraft upon the Atmosphere. Proc. Intern. Sci. Colloquium, Köln, 18.–20.4.1994, DLR-Mitt. 94-06, 430–435.

Brasseur, G. P., R. A. Cox, D. Hauglustaine, I. Isaksen, J. Lelieveld, D. H. Lister, R. Sausen, U. Schumann, A. Wahner, P. Wiesen, 1998: European Scientific Assessment of the Atmospheric Effects of Aircraft Emissions. — Atmos. Environ. **32**, in press.

Gibson, J. K., P. Kållberg, S. Uppala, A. Hernandez, A. Nomura, E. Serrano, 1997: ERA Description. — ECMWF Re-Analysis Project Rep. Ser. **1**, 1–72.

Gierens, K. M., 1996: Numerical simulations of persistent contrails. — J. Atmos. Sci. **53**, 3333–3348.

Goodman, R., 1988: Introduction to Stochastic Models. — Benjamin/Cummings, Menlo Park (California), 368 pp.

Konopka, P., 1995: Analytical Gaussian solutions for anisotropic diffusion in linear shear flow. — J. Non-Equilib. Thermodyn. **20**, 78–91.

Kuhn, P. M., 1970: Airborne observations of contrail effects on the thermal radiation budget. — J. Atmos. Sci. **27**, 937–942.

Mannstein, H., 1996: Contrail observations from space using NOAA-AVHRR data. — Proc. International Colloquium on Impact of Aircraft Emissions upon the Atmosphere, Paris, 15–18 Oct. 1996, 427–432.

Mannstein, H., R. Meyer, P. Wendling, 1997: Operational detection of contrails from NOAA-AVHRR-data. — DLR, Institut für Physik der Atmosphäre, Rep. No. 92, 18 pp.

Minnis, P., J. K. Ayers, S. P. Weaver, 1997: Surface-Based Observations of Contrail Occurrence Frequency Over the U.S., April 1993–April 1994. — NASA Reference Publ. 1404.

Minnis, P., D. F. Young, L. Nguyen, D. P. Garber, W. L. Smith, Jr., R. Palikonda, 1998: Transformation of contrails into cirrus during SUCCESS. — Geophys. Res. Lett., in press.

Ponater, M., S. Brinkop, R. Sausen, U. Schumann, 1996: Simulating the global atmospheric response to aircraft water vapour emissions and contrails — a first approach using a GCM. — Ann. Geophysicae **14**, 941–960.

Sausen, R., K. Gierens, M. Ponater, U. Schumann, 1998: A diagnostic study of the global potential coverage by contrails, Part I: Present day climate. — Theor. Appl. Climat., submitted.

Schmidt, E., 1941: Die Entstehung von Eisnebel aus den Auspuffgasen von Flugmotoren. — Schriften der Deutschen Akademie der Luftfahrtforschung, Verlag R. Oldenbourg, München und Berlin, H. 44, 1–15.

Schmitt, A., B. Brunner, 1997: Emissions from aviation and their development over time. — In: Schumann, U., A. Chlond, A. Ebel, B. Kärcher, H. Pak, H. Schlager, A. Schmitt, P. Wendling (Eds.): Pollutants from Air Traffic — Results of Atmospheric Research 1992–1997. DLR-Mitt. 97–04, 37–52.

Schumann, U., 1996: On conditions for contrail formation from aircraft exhausts. — Meteorol. Z., N.F. **5**, 4–23.

Schumann, U., P. Konopka, R. Baumann, R. Busen, T. Gerz, H. Schlager, P. Schulte, H. Volkert, 1995: Estimate of diffusion parameters of aircraft exhaust plumes near the tropopause from nitric oxide and turbulence measurements. — J. Geophys. Res. **100**, 14147–14162.

Schumann, U., P. Konopka, 1994: A simple estimate of the concentration field in a flight corridor. — In: Schumann, U., D. Wurzel (Eds.): Impact of Emissions from Aircraft and Spacecraft upon the Atmosphere. Proc. Intern. Sci. Colloquium, Köln, 18.–20.4.1994, DLR-Mitt. 94-06, 354–359.

Schumann, U., P. Wendling, 1990: Determination of contrails from satellite data and observational results. — In: Schumann, U., (Ed.): Air Traffic and Environment, 138–153, Springer-Verlag.

Dr. KLAUS GIERENS
Deutsches Zentrum für Luft- und Raumfahrt (DLR) e.V.
Institut für Physik der Atmosphäre
Oberpfaffenhofen
D-82234 Weßling
e-mail: klaus.gierens@dlr.de

Received 26 August 1997, in revised form: 15 December 1997